Accepted Astrophysical Journal, Jul 19, 2010

A Spitzer Search For Planetary-Mass Brown Dwarfs With Circumstellar Disks: Candidate Selection

Paul M. Harvey[1], Daniel T. Jaffe[1] Katelyn Allers[2], Michael Liu[3]

ABSTRACT

We report on initial results from a *Spitzer* program to search for very low-mass brown dwarfs in Ophiuchus. This program is an extension of an earlier study by Allers et al. which had resulted in an extraordinary success rate, 18 confirmed out of 19 candidates. Their program combined near-infrared and Spitzer photometry to identify objects with very cool photospheres together with circumstellar disk emission to indicate youth. Our new program has obtained deep IRAC photometry of a 0.5 deg^2 field that was part of the original Allers et al. study. We report 18 new candidates whose luminosities extend down to 10^{-4} L$_\odot$ which suggests masses down to $\sim 2\ M_J$ if confirmed. We describe our selection techniques, likely contamination issues, and follow-on photometry and spectroscopy that are in progress.

Subject headings: planetary systems: protoplanetary disks stars: formation stars: low-mass, brown dwarfs

1. Introduction

Young brown dwarfs exhibit "circumstellar" disk phenomena much like their more massive counterparts, e.g. (Apai et al. 2004), (Luhman et al. 2010). Although there are quantitative differences in detailed physical parameters for disks around sub-stellar objects

[1]Astronomy Department, University of Texas at Austin, 1 University Station C1400, Austin, TX 78712-0259; pmh@astro.as.utexas.edu, dtj@astro.as.utexas.edu

[2]Department of Physics and Astronomy, Bucknell University, Lewisburg, PA 17837; k.allers@bucknell.edu

[3]Institute for Astronomy, University of Hawaii, 2680 Woodlawn Dr., Honolulu, HI 96822; mliu@ifa.hawaii.edu

(Pascucci et al. 2009), the distribution of disk properties appears to be relatively continuous across the sub-stellar boundary, e.g. Scholz et al. (2009). The lower limit to the sub-stellar mass of objects that form with accretion disks is, however, still uncertain. Theoretical considerations of the opacity limit for fragmentation of clouds, e.g. Bate (2009), suggest that such a formation mechanism is likely to be limited to central objects above a few Jupiter masses (M_J). In recent years a number of studies have been made to push the detection limit on low-mass brown dwarfs to the lowest possible levels, in part to test these theoretical predictions. In general, these studies have taken advantage of the fact that young BD's are significantly more luminous and detectable than older field BD's, and thus these investigations have focussed on star-forming regions. Infrared excesses due to circum-object material provide an additional discriminant to isolate young brown dwarfs, as well as a tool to investigate the properties of disks around such cool, low-mass central objects.

One of the most successful searches for young, low-mass BD's was that of Allers et al. (2006), hereafter A06. Since the original publication of their 19 candidates, Allers et al. (2007) and Gully-Santiago et al. (2010) have spectroscopically confirmed 18 out of the 19 candidates as low-mass stars and sub-stellar objects. A06 used a combination of color and magnitude criteria to select objects with the properties of cool, low-luminosity sub-stellar objects in fields observed by the Spitzer *c2d* Legacy program (Evans et al. 2003). The Spitzer data provided the ability to search for infrared excesses, presumably due to circumstellar disks, which would imply youth and membership in the star-forming clouds. The observational limit on low-luminosity objects in their study was set by the *c2d* sensitivity in the two longest wavelength Spitzer IRAC bands at 5.8 and 8.0μm, a result of the relatively short integration times of 48 sec required by the large area survey.

We report here on a program of much deeper Spitzer imaging of a 0.5 deg^2 area in the Ophiuchus star-forming region where matching, deep I, J, H, and K_s photometry already exist from the original A06 study. Our program was aimed at detecting young, planetary-mass objects down to masses of 2 M_J with circumstellar disks. The youngest YSOs in the core of Ophiuchus are probably under 1 Myr in age, but star formation appears to have been underway for 2 - 5 Myr in the more extended area surveyed in our study (Wilking, Gagné & Allen 2008). In addition to testing the opacity limit for fragmentation and the lower limit of the IMF, detection of a number of such objects would provide a sample to: 1) study the properties of disks physics in an extended range of temperature and gravity parameter space; 2) probe the atmospheres of the lowest mass 1 Myr old BD's; 3) test the $\dot{M}/M_*$ relation to lower masses; and 4) examine the distribution and multiplicity of very low mass objects for hints to their origin. In this first paper, we focus on objects that were pre-selected from the IJHK data to meet all the selection criteria of A06 for the faintest magnitude bin. We then examined our observations of these objects to search for examples with IRAC excesses.

In §2 we describe the details of our Spitzer observations and data reduction processes. We then discuss how we have selected our candidate objects in §3. In §4 we discuss the kinds and number of contaminants that we expect in our sample and finally mention followup observations that are planned to investigate the reliability of this sample.

2. Observations and Data Reduction

Table 1 lists the AOR's that were part of this Spitzer program PID 50025. The total integration time per pixel was roughly 900 sec in all four IRAC bands. The three shorter wavelength bands were observed with 100 sec frame times, while band 4 (8.0μm) was observed with 50 sec frame times.

We used most of the features of the *c2d* pipeline (Evans et al. 2007) to process the data. We did not, however, use any additional masking beyond the recommended mask bits in the IRAC data handbook[1], and band-merging was accomplished with a simple positional-matching algorithm, i.e. positional coincidence within 2 arcsec. Sources with any significant confusion were hand-checked to be sure the matches were reliable. The frames were mosaicked with the standard version of the Spitzer mosaicker, Mopex, with the output pixel size set to be equal to the input pixel size. The *c2d* source extraction tool, c2dphot (Evans et al. 2007), was used in several different modes to extract sources and measure fluxes. For most of the objects we used the standard mode of extraction from the full mosaic at each wavelength, and then flux measurement from the stack of individual BCD's appropriate for each source. For a few of the final selected sources, the level of diffuse background was so high, that even with the PSF-fitting used by c2dphot, we were unable to extract a source at 5.8 or 8μm. In these cases we used the tool in a mode where the position was held fixed at the source position determined from the IRAC band 1 and 2 extractions while the flux was determined from a PSF-fit. Tests we have done show that this can underestimate the true flux by order up to 20% because the position is not allowed to vary during the fitting. In any case, the fluxes of all these fixed-position sources have relatively high uncertainties due to the high background. Since these two longest wavelengths were used to search for circumstellar excess in our program, the underestimate of the fluxes means that our final list of excesses is likely to be slightly conservative if anything.

[1]http://ssc.spitzer.caltech.edu/irac/iracinstrumenthandbook/home/

3. Candidate Selection

The goal of this first part of our study was to look specifically at objects in Ophiuchus that had been selected by the criteria in A06 for the faintest magnitude bins and which were lacking IRAC detections at 5.8 and 8.0μm due to the modest integration times of the *c2d* survey. Using those criteria resulted in a list of 605 objects in the area covered by A06 at I–K_S. Of these, 549 were in the area covered by our new Spitzer observations at both 5.8 and 8.0μm and 578 were covered at 5.8μm. Of these, 179 sources were bright enough for successful flux extraction. The existing A06 shorter wavelength data were then band-merged with our new photometry for these sources. In a future study we will take a broader look at our photometry beyond this first set of candidates.

In order to search for candidate objects with an infrared excess, it is of course necessary to know the colors/magnitudes of comparable objects without an excess. This may be problematic, however, since we cannot know for sure what the atmospheres of such low-mass brown dwarfs look like. Since the A06 study, Patten et al. (2006) have published an extensive set of Spitzer photometry of field brown dwarfs as late as spectral type T8. Roughly speaking, we would expect that a young few M_J object would have a spectral type of mid- to late-L (Burrows et al. 1997), but would likely be more luminous than older field dwarfs of the same spectral type. Objects near the deuterium-burning limit, M $\sim$ 15 M_J, for comparison would have luminosities $\sim 10^{-3}$ $L_\odot$, and spectral types of late M to early L for roughly the first 10 Myr of their lifetimes (Burrows et al. 1997; Chabrier et al. 2000). (Of course, recent theoretical investigations have shown that the accretion history of young, low-mass objects can make the correspondence between mass and observable quantities highly problematic (Baraffe, Chabrier & Gallardo 2009)). We have, therefore, developed two additional selection criteria beyond those of A06, to select objects with shorter wavelength colors appropriate for planetary-mass BD's and longer wavelength colors implying an excess above that expected for known field dwarfs. These selection criteria are illustrated in Figures 1 and 2.

In Figure 1, we have plotted the absolute K_S magnitude versus the observed I–K_S color for a variety of objects. We chose this color-magnitude pair because at I and K_S there should be little excess emission from circumstellar disks, and the colors of field dwarfs listed by Patten et al. (2006) and Caballero, Burgasser & Klement (2006) are nearly monotonic with spectral type in these bands. The absolute magnitudes of observed objects in Ophiuchus have been calculated assuming a distance modulus of 5.48 mag. We have used this diagram for two purposes: 1) to provide an additional color-magnitude selection of objects with colors of cool sub-stellar objects, but with magnitudes brighter than the older field dwarfs of Patten et al. (2006), and 2) to estimate conservative values for the reddening to our candidates in order to

more accurately select objects with longer wavelength excesses. The solid, somewhat wavy black line shows the colors and magnitudes for the field dwarfs of Patten et al. from M3 to L7. The large open triangles show the locations in this diagram for the 19 candidates of A06 (the one that was, in fact, extragalactic is noted by a large overlying "X"). The green circle shows the approximate location for the 2 M_J disk-less model described in A06.

We used the combination of the Patten et al. data and the Allers et al. candidates to set two, somewhat arbitrary, limits on the figure. The upper dot-dash line shows our assumed color-magnitude relation for diskless, very young low-mass brown dwarfs in order to estimate reddening to our objects. We chose this line simply by the fact that it is roughly a magnitude brighter at all colors than the field dwarf relationship, and is at the bottom of the distribution of colors/magnitudes of the confirmed objects from A06. We believe this to be a conservative estimate of intrinsic colors in the sense that it probably provides an upper limit to the actual interstellar extinction; indeed, spectroscopic confirmation of the brightest of our candidates (Allers & Liu 2010) finds a reddening somewhat less than that estimated from this simple relation. The extinction values listed in Table 2 were derived by dereddening our observed colors back to this line. The lower, dashed, line shows our cutoff for selection of candidates in this color-magnitude space. This line was set, again somewhat arbitrarily, at about a half magnitude brighter than the field dwarf relation in order to select for young, i.e. larger diameter objects. In addition, as described in the figure, we show the positions of the final selected candidates as well as objects that were rejected, either because of their position in this diagram or Figure 2, or because they appeared to be extended in one of the images.

Figure 2 shows our selection criterion aimed at choosing objects with some excess emission in the longer IRAC bands to pick out objects with circumstellar disks, which would then be more likely to be young objects in the Ophiuchus star-forming cloud. We decided to use the 5.8μm photometry as a measure of disk excess rather than the 8.0μm values because a significant number of our candidates were surrounded by enough diffuse (presumably PAH) emission that extracting good photometry at 8.0μm was highly problematic. The symbols have the same meaning as in the preceding figure (Figure 1). The colors and magnitudes have been dereddened using the extinction derived from Figure 1 which is also listed in Table 2. We assumed the same extinction dependence on wavelength as A06 for consistency. In this diagram we selected any object that was more than 0.1 magnitude redder than the relation shown for the field dwarfs of Patten et al. Note, in this color-magnitude space the extragalactic interloper in the A06 study is significantly redder than any of the low-mass brown dwarfs, while in Figure 1 it is bluer, and in fact would have been eliminated by these new selection criteria.

After applying both of these color-magnitude criteria to the 179 objects that were detected at 5.8μm out of the initial 605 candidates and eliminating any objects that appeared extended in either the I or 3.6μm images, we were left with 18 new final candidates; these are listed in Table 2. Their luminosities were derived by integrating the dereddened spectral energy distributions from I through 8μm assuming the extinctions listed. In the following section we discuss the probability that this list actually contains examples of planetary-mass young brown dwarfs.

Although our study is essentially an extension of that by A06, there *are* a few small differences in our selection criteria. Since we started with a list of sources that fit the A06 selection criteria in the I thru 3.6μm bands, that part of the selection is identical. For selection of sources with shorter wavelength colors of sub-stellar objects, however, our criteria were more stringent with the addition of the color-magnitude cuts shown in Figure 1. In principle this should result in a lower likelihood of contamination by extragalactic objects; we discuss this issue in more detail in the following section. The second difference is that A06 insisted on a 3-sigma excess at both 5.8 and 8μm over the colors of field M dwarfs. Our criterion shown in Figure 2 is somewhat looser in that: 1) we have only used the 5.8μm excess, and 2) for the 2 sources closest to the cutoff line the excess only amounts to roughly 1σ.

4. Discussion

4.1. Contamination

There are a variety of objects other than very low mass young BD's that may contaminate our sample by mimicing the color/magnitude criteria that we have used in our selection.. These include: foreground or background dwarfs, extragalactic objects, particularly AGN, and distant background evolved stars. Here we examine the likelihood of contamination by each of these.

We have specifically chosen color and color-magnitude selection criteria that have worked very well to pick out cool dwarfs in the A06 study. One consequence of this selection scheme is that the most likely contaminants may be foreground and background cool stars. It is relatively easy to eliminate background giants as likely contaminants because of the galactic latitude of our survey field, 18°. Any red giant with apparent magnitudes comparable to our selection criteria would be at a distance of at least 20 kpc, and 7 kpc above the Galactic Plane. Low-mass field stars and BD's in the foreground and near-background will, of course, have colors and magnitudes much closer to those of our selected objects with the

exception of the longer IRAC bands. Caballero, Burgasser & Klement (2006) have published a procedure for estimating exactly this sort of contamination in searches such as ours. The situation for Ophiuchus is somewhat more favorable than for the other two cases examined by Caballero, Burgasser & Klement (2006), Orion and the Pleiades, because both the Sun and the cluster are on the same side of the Galactic plane so we never look through the plane. Using the prescription given by Caballero, Burgasser & Klement (2006) it is clear that foreground contamination is not an issue, since such objects would necessarily be lower luminosity BD's than those in the star-forming cloud, and such objects are not numerous. In our survey area, we would expect of order one such foreground field dwarf contaminant. Background BD's and M dwarfs are a more serious problem, since a background M5 dwarf with a few magnitudes of visual extinction would have colors and magnitudes comparable to our I/K selection criteria for a distance of a couple hundred pc. For example, using the algorithm of Caballero, Burgasser & Klement (2006) we estimate that of order 20 M dwarfs could occupy the area in Figure 1 defined by $9 < K_{abs} < 10, 4.5 < I - K < 5.5$. This area contains a number of our candidates as well as several tens of objects that we have discarded. The one criterion that background field dwarfs would not satisfy, of course, is that for an excess in the K-[5.8] colors shown in Figure 2.

Various extragalactic objects can, however, exhibit a very wide range in infrared excess. At the faintest magnitudes within even the Spitzer *c2d* survey, the most serious contaminants are the extragalactic objects, e.g. (Harvey et al. 2007). The IRAC magnitude limits reached in our survey are comparable to those of the Spitzer *SWIRE* legacy survey (Lonsdale et al. 2004); the color-magnitude distribution of these sources in the IRAC bands as shown in Figure 3 of Harvey et al. (2007) covers a wide range, making them very hard to eliminate with Spitzer data alone. The SWIRE survey *has* acquired deep I-band photometry of their fields, though unfortunately not matching JHK photometry. We can examine the possible contamination of our sample by extragalactic sources by comparing our sample colors and magnitudes with those of the SWIRE sample in bands that do overlap. Figure 3 shows such a comparison using the I, [3.6], and [5.8] bands. The particular sample we have selected via the IRSA Gator search engine[2] was chosen to minimize the presence of extended sources. In particular, we chose objects with a "stellarity index" less than unity and a difference between aperture magnitude and integrated magnitude in the I band less than 0.3. As described in the figure, we show both the full data set for the ElaisN1 field ~ 8.5 deg^2, and a randomly selected subsample diluted by the ratio of the area of our survey, 0.5 degree. It is clear from the [3.6] vs I-[3.6] diagrams that the brightest 3/4 of our sample are unlikely to be contaminated by extragalactic objects. The fainter few objects, though, are located in

[2]http://irsa.ipac.caltech.edu/applications/Gator/

regions of both color-magnitude diagrams where there is a high concentration of extragalactic sources. Spectroscopy will be needed to ascertain which of these is stellar, though our preliminary work with [1.45]-filter photometry described below shows that at least some of our candidates are likely to be cool, low-luminosity objects.

A final very qualitative tool to investigate contamination is to compare the spatial distribution of the well-vetted A06 sample of brighter low-mass BD's and M dwarfs with our new sample of candidate lower mass objects. Figure 4 shows just such an image. There is no obvious difference in the degree of clustering or distribution within the field of the two samples. Of course, with the relatively small number of objects in both samples, this is not surprising.

4.2. Verification Plans

We have initiated several programs to determine the extent to which our new candidates do represent very low-mass sub-stellar objects. The first of these programs is described by Allers & Liu (2010) who have developed a narrow-band filter, the "[1.45]" filter, to identify objects with strong H_2O absorption in the H-band spectral region, indicative of very low temperature photospheres. These data are still being analyzed, but some preliminary results have shown that four of our candidates do indeed fit the classification as low-photospheric-temperature objects characteristic of low-mass BD's. These objects have been indicated in Figures 1, 2, and 3 by red circles. An additional 46 objects have been identified as [1.45]-absorption candidates in our field; these were either not detected at 5.8μm or did not meet our selection criteria.

In a second program we have been awarded time on the VLT with the X-shooter spectrograph to obtain moderate resolution spectra of the five faintest candidates in Table 2. And finally, in a collaborative program with A. Goodman, we are hoping to obtain spectra of a number of brighter candidates with GNIRS in the near future. These results will also be reported in forthcoming publications.

5. Summary

From an initial sample of 605 objects in Ophiuchus that were selected by the original A06 photometric criteria between I and 3.6μm, we have identified 18 candidates that have near-infrared magnitudes and colors consistent with very cool sub-stellar photospheres together with possible 5.8μm excesses that would be consistent with circum-object disk emission.

Our sample extends the work of A06 to luminosities of 10^{-4} $L_{\odot}$, a factor of 10 below their limits. Contamination by background field dwarfs in the brighter magnitude range of our sample and by extragalactic objects at the fainter magnitudes is likely to be significant. It is certainly possible that at least half of our candidates are such contaminants. Narrow-band filter photometry in progress, however, has shown that at least several of our candidates are likely to be low-mass BD's with circum-object disks. It is likely that further candidates exist in our data set, though problems with diffuse 5.8 and 8μm emission in the region make it difficult to clearly confirm many more disk candidates.

6. Acknowledgments

Support for this work was provided by NASA through RSA 1281173 issued by the Jet Propulsion Laboratory, California Institute of Technology, to the University of Texas at Austin and NASA Origins grant NNX07AI83G to the University of Texas. P. Harvey thanks the Laboratoire Astrophysique de l'Observatoire de Grenoble (LAOG) for its gracious support during a sabbatical while much of this research was performed.

Table 1: Observations Summary (Program ID = 50025)

AOR	Date	AOR Type	BCD Process
ads/sa.spitzer#0025243648	2009-04-24	IracMap	S18.7.0
ads/sa.spitzer#0025243904	2009-04-22	IracMap	S18.7.0
ads/sa.spitzer#0025244160	2009-04-23	IracMap	S18.7.0
ads/sa.spitzer#0025244416	2009-04-25	IracMap	S18.7.0
ads/sa.spitzer#0025244928	2009-04-25	IracMap	S18.7.0
ads/sa.spitzer#0033970176	2009-04-25	IracMap	S18.7.0
ads/sa.spitzer#0033970432	2009-04-23	IracMap	S18.7.0

Table 2. Photometry of Selected Candidates

Position	I mag	J mag	H mag	K_s mag	3.6 μm mag	4.5 μm mag	5.8 μm mag	8.0 μm mag	A_v mag	Luminosity Log ($L_\odot$)
16 21 23.94 -24 00 19.8	21.08±0.05	17.53±0.03	16.52±0.03	15.94±0.03	15.24±0.05	15.11±0.05	14.97±0.08	14.47±0.11	0.0	-3.6
16 21 53.36 -23 40 19.2	23.61±0.11	19.31±0.06	17.94±0.04	17.29±0.05	16.40±0.05	16.26±0.05	15.92±0.19	16.38±0.81	0.7	-4.1
16 22 20.40 -23 07 52.3	21.74±0.05	16.82±0.19	15.42±0.13	14.89±0.12	14.11±0.05	···	13.66±0.05	···	6.2	-2.8
16 22 24.73 -23 26 20.2	19.98±0.05	16.53±0.03	15.60±0.03	15.03±0.03	14.58±0.05	14.42±0.05	14.07±0.06	13.77±0.13	0.7	-3.2
16 22 26.70 -23 08 53.3	20.28±0.05	16.79±0.19	15.39±0.11	14.92±0.14	14.41±0.05	···	13.95±0.17	···	2.1	-3.1
16 22 31.60 -23 10 15.2	19.72±0.05	16.30±0.12	15.35±0.10	14.65±0.11	14.24±0.13	···	13.92±0.07	···	1.7	-3.0
16 22 35.46 -24 13 22.2	19.83±0.05	16.59±0.14	15.93±0.14	15.13±0.18	14.67±0.05	14.72±0.05	14.15±0.10	14.03±0.14	0.0	-3.3
16 22 50.26 -23 09 47.7	19.89±0.05	16.47±0.15	15.56±0.13	15.10±0.17	14.48±0.05	···	14.01±0.10	···	0.2	-3.2
16 22 52.60 -23 18 07.8	19.23±0.05	15.79±0.03	15.08±0.03	14.71±0.13	14.21±0.05	14.04±0.05	13.89±0.05	13.75±0.07	0.1	-3.0
16 22 52.77 -23 30 49.1	20.47±0.05	16.78±0.19	15.72±0.14	15.13±0.16	14.59±0.05	14.43±0.05	14.20±0.06	14.51±0.20	1.6	-3.2
16 22 56.08 -24 14 31.2	20.19±0.05	16.49±0.13	15.66±0.10	14.96±0.15	14.49±0.05	14.33±0.05	14.08±0.08	14.29±0.15	1.6	-3.1
16 22 56.11 -23 16 12.1	20.93±0.06	16.81±0.18	15.77±0.14	15.44±0.21	14.73±0.05	14.56±0.05	14.40±0.07	14.99±0.37	1.5	-3.2
16 23 15.15 -23 47 05.1	19.58±0.05	15.12±0.03	14.20±0.03	13.52±0.03	12.95±0.05	12.73±0.05	12.53±0.05	12.44±0.05	6.4	-2.2
16 23 19.28 -23 33 40.6	19.95±0.05	16.43±0.12	15.69±0.12	15.20±0.16	14.54±0.05	···	14.22±0.06	···	0.0	-3.2
16 23 33.66 -23 52 36.5	22.95±0.07	19.04±0.05	17.96±0.04	17.24±0.04	16.65±0.05	16.31±0.06	15.38±0.15	14.13±0.21	0.0	-4.1
16 23 33.74 -23 48 37.2	23.60±0.10	19.26±0.06	18.19±0.04	17.39±0.04	16.56±0.06	16.43±0.06	15.62±0.19	···	0.2	-4.2
16 23 36.49 -23 44 04.8	20.39±0.05	16.60±0.16	15.21±0.09	15.19±0.20	14.21±0.05	14.07±0.05	13.98±0.06	14.17±0.16	1.2	-3.1
16 23 46.86 -23 36 38.1	19.37±0.05	15.84±0.09	14.92±0.07	14.43±0.10	13.74±0.05	···	13.35±0.05	···	1.8	-2.8

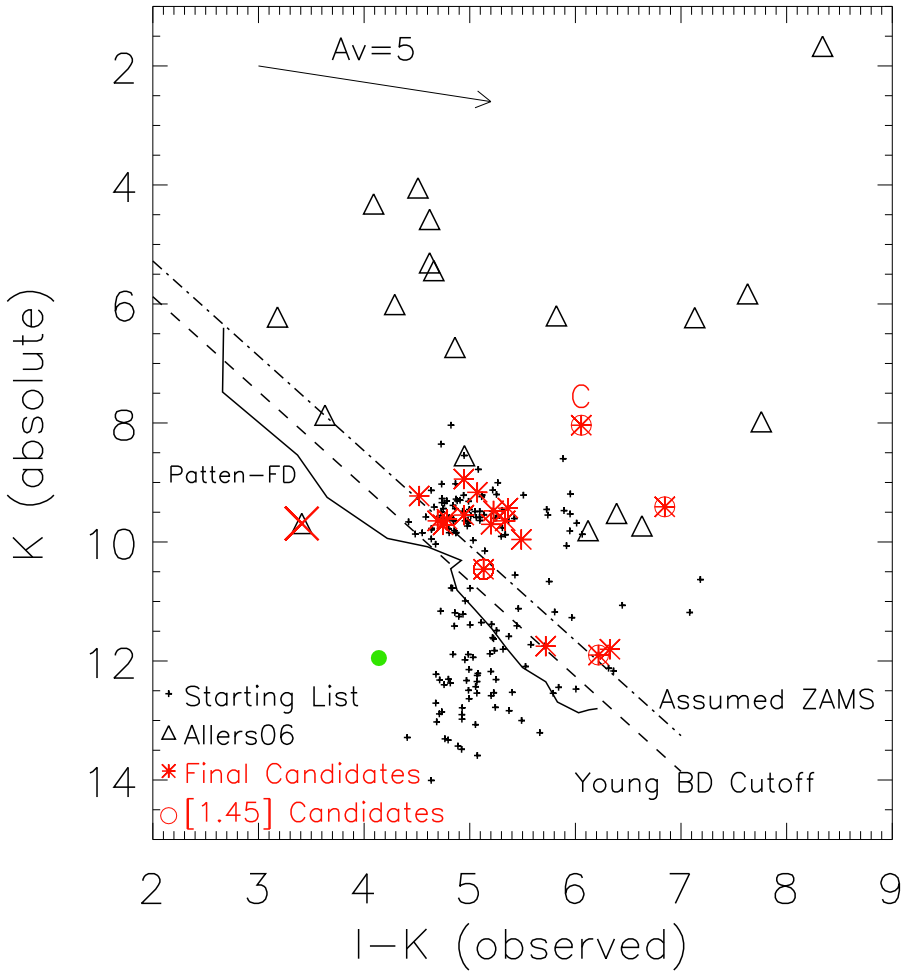

Fig. 1.— Absolute K_S magnitude versus I – K_S color (assuming a distance of 125pc for all objects). Our final selected candidates are marked with red asterisks; the 161 candidates out of our starting list of 179 candidates that did not meet all the selection criteria are marked by small crosses; objects that were found by Allers and Liu (2010) with likely water absorption in the near-infrared are marked with red circles; the one source in our candidate list that has already been spectroscopically confirmed is marked also with a "C"; and the locations in this diagram of the original A06 candidates are marked with black triangles. The one source from A06 that was found to be extragalactic is overlaid with a large red "X". A solid green circle shows the approximate location in this color-magnitude space of the 2 M_J diskless model from A06. The solid line shows the distribution of field dwarfs in this color-magnitude space from Patten et al. (2006) and Caballero, Burgasser & Klement (2006). The dash-dot line is a straight line about 1 mag brighter than the Patten distribution, which we chose as a probable distribution for unreddened young brown dwarfs in order to estimate the interstellar reddening to our candidates. The dashed line below that marks our limit in this color-magnitude space for selecting objects in our final candidate list that also fit our other selection criteria.

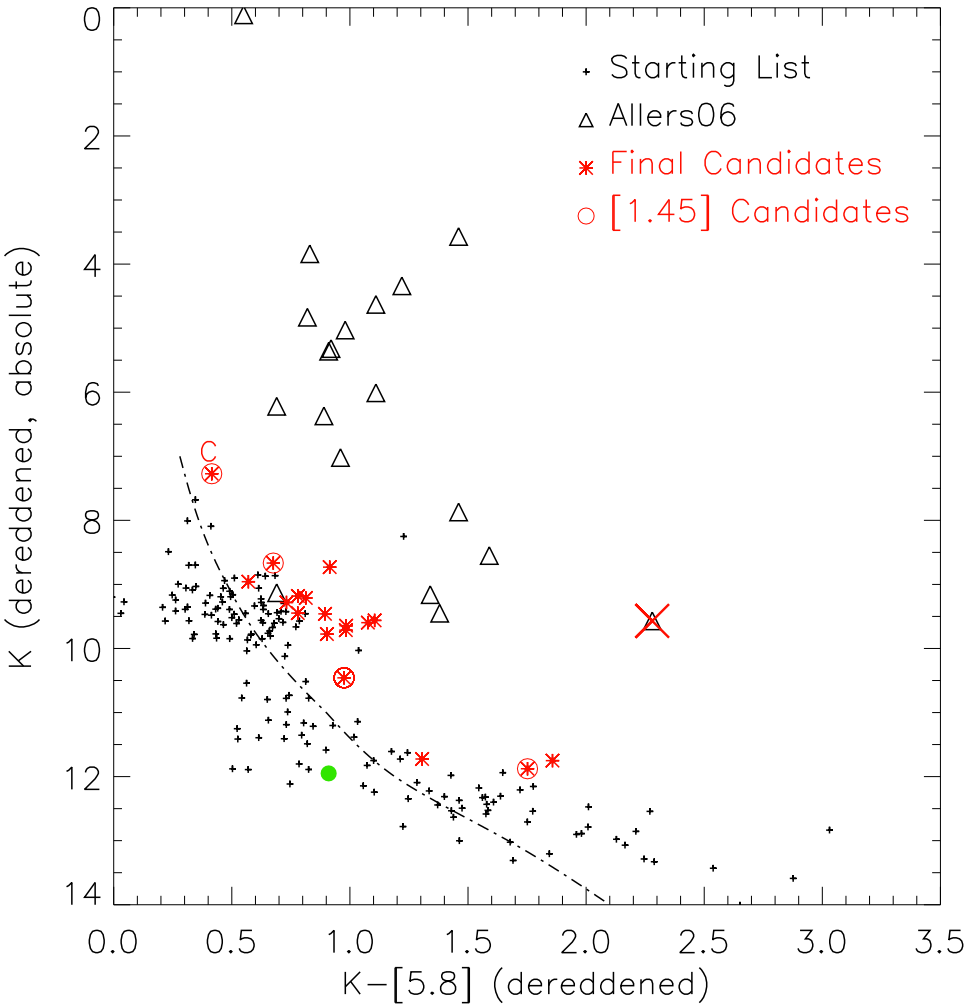

Fig. 2.— Absolute dereddened K_S magnitude versus dereddened K_S – [5.8] color as described in the text. The symbols are the same as in Fig. 1. The dash-dot line shows the rough distribution of field dwarfs in this color-magnitude space from Patten et al. (2006). This diagram was used to select sources with possible disk emission by choosing sources at least 0.1 mag above the dash-dot line that also met our other criteria.

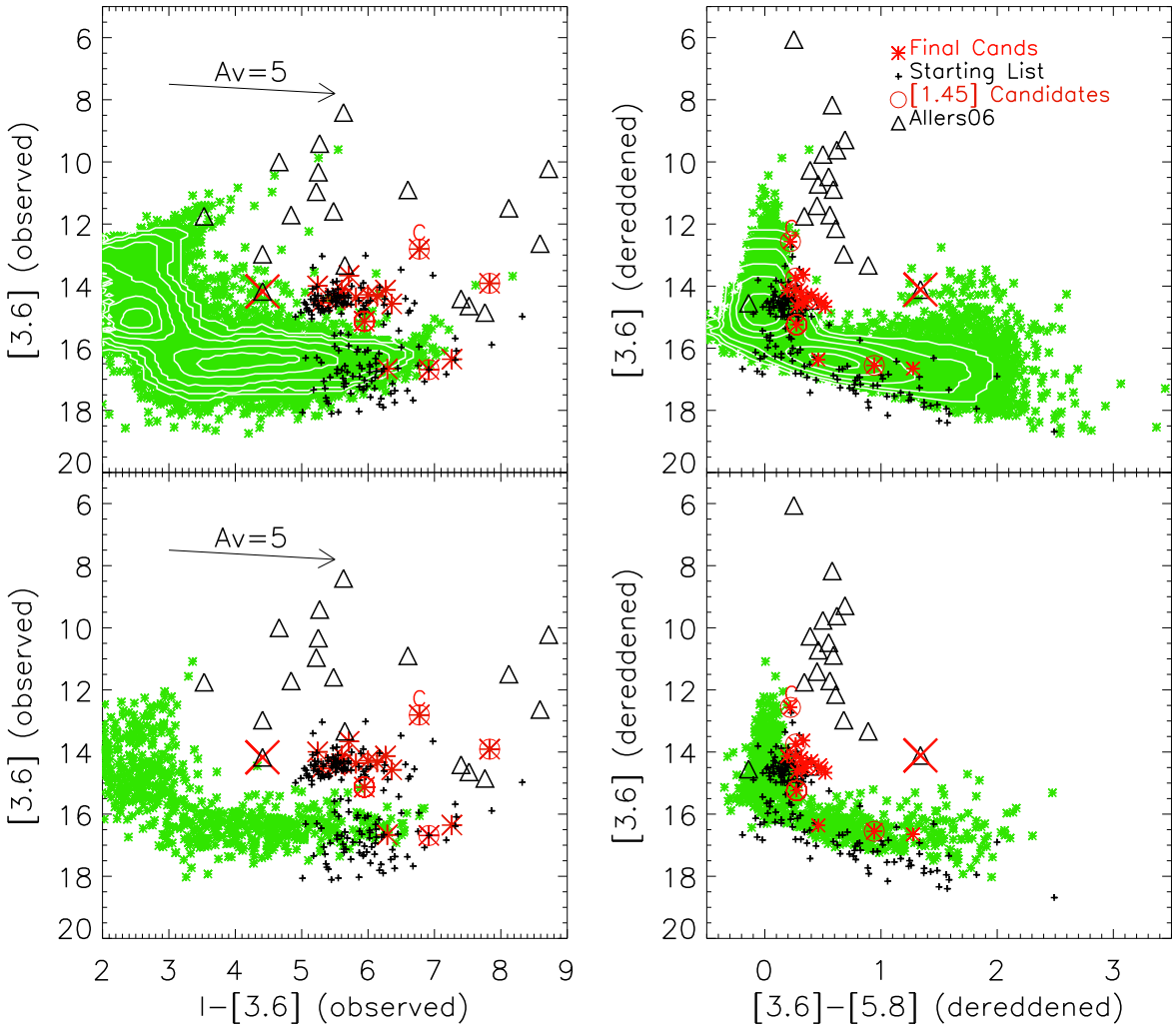

Fig. 3.— Color magnitude diagrams showing the locations of our final candidates, as well as the original list from which we selected these, and the corresponding colors/magnitudes from the A06 study. The objects that fit the [1.45]-filter selection described in the text for M dwarfs are surrounded by red circles. Objects from the Elais N1 field of the SWIRE Spitzer Legacy program are shown in green; the upper panels show the full sample, while the lower ones show a sub-sample with the number of randomly selected objects normalized by the ratio of the area of our sample to that of the SWIRE Elais N1 field. The white contours in the upper panels are at levels of 5, 10, 20, 40, 60, and 80 percent of the peak density of extragalactic points. The peak levels are 24 per 0.1 mag bin in each axis in the upper left diagram and 76 per 0.1 mag bin in each axis in the upper right diagram.

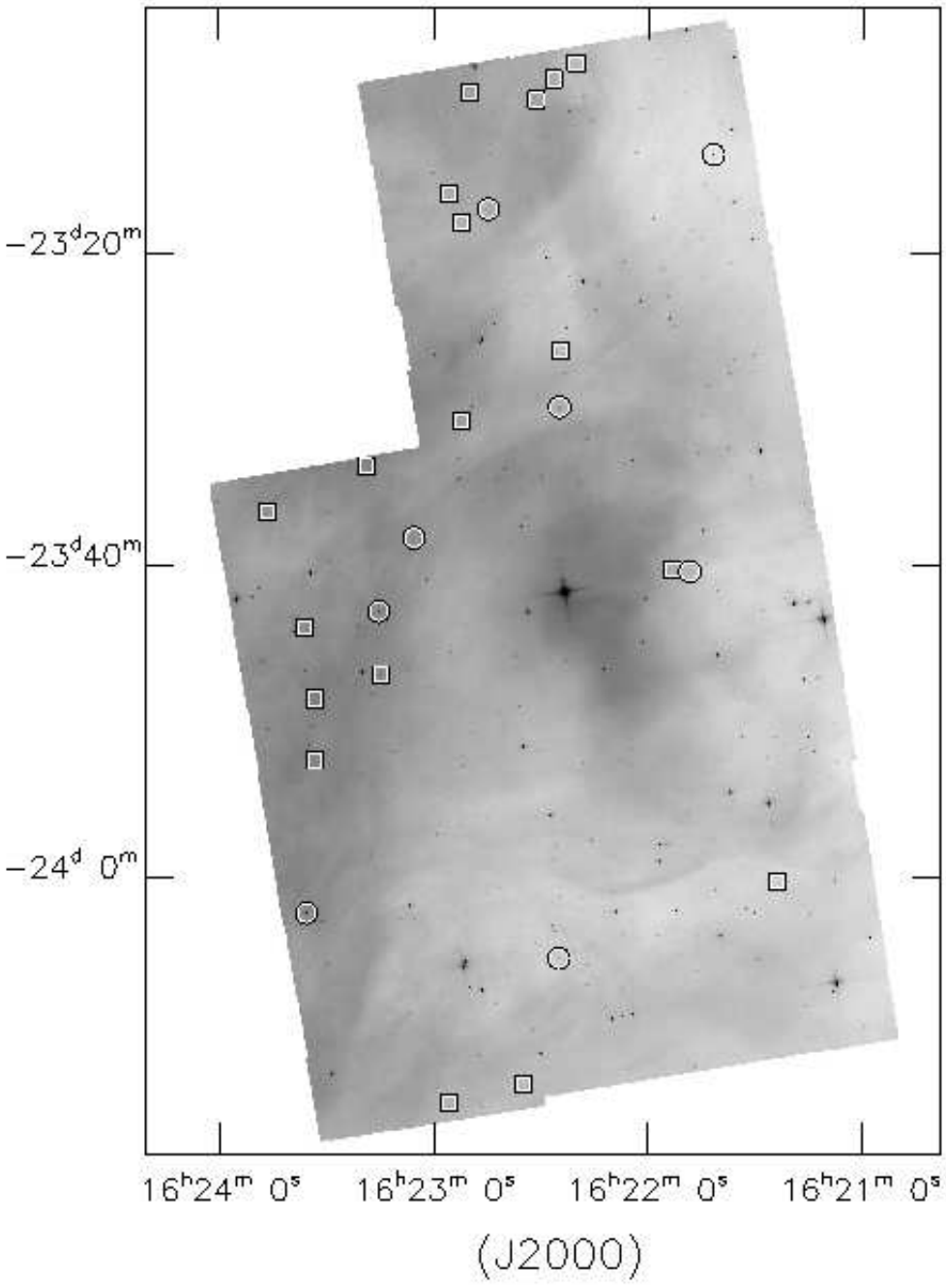

Fig. 4.— Distribution of new candidate sources (boxes) and verified low-mass BD's from A06 (circles) within our deep Spitzer search area.

REFERENCES

Allers, K. N., Kessler-Silacci, J. E., Cieza, L. A. & Jaffe, D. T. 2006, ApJ, 644, 364

Allers, K. N. et al. 2007, ApJ, 657, 511

Allers, K. N. & Liu, M. C. 2010, BAAS, 42, 335

Apai, D. et al. 2004, A&A, 426, L53

Baraffe, I., Chabrier, G. & Gallardo 2009, ApJ, 702, L27

Bate, M. R. 2009, MNRAS, 397, 232

Burrows, A. et al 1997, ApJ, 491, 856

Caballero, J. A., Burgasser, A. J. & Klement, R. 2006, A&A, 488, 181

Chabrier, G., Baraffe, I., Allard, F. & Hauschildt, P. H. 2000, ApJ, 542, 464

Evans, N. J., II, et al. 2003, PASP, 115, 965

Evans, N. J., II et al. 2007, Final Delivery of Data From the c2d Legacy Project: IRAC and MIPS, http://data.spitzer.caltech.edu/popular/c2d/20071101_enhanced_v1/ Documents/c2d_del_document.pdf

Gully-Santiago, M. et al 2010, in prep.

Harvey, P. M. et al 2007, ApJ, 663, 1149

Lonsdale, C. et al. 2004, ApJS, 154, 54

Luhman, K.L., Allen, P.R., Espaillat, C., Hartmann, L. & Calvet, N. 2010, ApJS, 186, 111

Pascucci, I. et al. 2009, ApJ, 696, 143

Patten, B. M. et al. 2006, ApJ, 61 502

Scholz, A., Geers, V., Jayawardhana, R., Fissel, L., Lee, E., LaFreniere, D. & Tamura, M. 2009, ApJ, 702, 805

Wilking, B. A., Gagné, M. & Allen, L. E. 2008, in Handbook of Star Forming Regions, Vol. 2, ed. B. Reipurth (San Francisco: ASP), pp. 351380